SCIENCE CHINA
Technological Sciences

•Article•

September 2019 Vol.62 No.9: 1605–1615
https://doi.org/10.1007/s11431-017-9307-5

Crack propagation mechanism of γ-TiAl alloy with pre-existing twin boundary

CAO Hui[1,2,3], RUI ZhiYuan[1,2,3*], CHEN WenKe[1,2,3], FENG RuiCheng[1,2,3] & YAN ChangFeng[1,2,3]

[1] *Engineering Research Center of Nonferrous Metallurgy's New Equipment, Ministry of Education, Lanzhou University of Technology, Lanzhou 730050, China;*
[2] *School of Mechanical and Electronical Engineering, Lanzhou University of Technology, Lanzhou 730050, China;*
[3] *State Key Laboratory of Advanced Processing and Recycling of Non-ferrous Metals, Lanzhou University of Technology, Lanzhou 730050, China*

Received December 13, 2017; accepted June 11, 2018; published online February 21, 2019

The deformation and failure mechanisms of γ-TiAl alloy with pre-existing crack and twin boundary are investigated by using molecular dynamics simulation. The effects of the crack position on the deformation and failure mechanisms of γ-TiAl specimen are analysed through the snapshots of crack propagation, microstructure of crack tip and stress-strain curves. The simulation results show that the dislocation motion is impeded, the good ductility can be maintained and the strength would be improved simultaneously by the twin boundary. The microstructure evolution of crack tip would change with crack positions. Essentially, the deformation behaviour mainly results from the reaction of dislocation-dislocation, dislocation-twin and twin-twin. Besides, the hierarchical twin is a main plastic deformation mechanism leading to strength of γ-TiAl specimen enhancement with non-compromising ductility and strain hardening. Based on stress-strain curves, it can be concluded that the yield strength varies with crack positions. They are the determinant factors for variation of the yield strength with different crack positions such as dislocation behaviour, stacking fault and hierarchical twin. The ductile-brittle transition associated with the dislocation motion and the decohesion failure of crack tip atom can be observed from the lower boundary crack and the center crack models. The crack propagation caused by the coalescent of the void and the crack tip is the main failure mechanism of γ-TiAl specimen. In addition, the results reveal that the mechanism of crack propagation would be influenced by pre-existing twin boundary which can prevent the crack propagation and improve the fracture toughness.

crack propagation, γ-TiAl, twin boundary, molecular dynamics, deformation mechanism

Citation: Cao H, Rui Z Y, Chen W K, et al. Crack propagation mechanism of γ-TiAl alloy with pre-existing twin boundary. Sci China Tech Sci, 2019, 62: 1605–1615, https://doi.org/10.1007/s11431-017-9307-5

1 Introduction

In recent years, TiAl alloy has been widely used in aviation and automobile industries as a high temperature metallic material because of its high capability such as low density, high stiffness, good flame retardant ability, corrosion resistance, high temperature creep resistance and so on [1–4]. The poor plasticity at room temperature restricts the application, since few slip systems exist in γ-TiAl alloy and they are difficult to slip [5]. Extensive efforts have been made to improve its plasticity at room temperature [6,7]. For example, polysynthetic twinned TiAl single crystals were fabricated using directional solidification methods by Chen et al. [7]. Their research results indicated that the alloy had well tensile ductility and yield strength at room temperature. When the temperature is higher, the yield strength remains

*Corresponding author (email: zhiy_rui@163.com)

high and tensile ductility better than that of room temperature, its mechanical properties would vary with lamellar orientation. This TiAl single-crystal alloy could provide expanded opportunities for higher temperature applications. Fowood's [8] experimental result showed that it was an effective method to improve the strength and plasticity by increasing the fraction of twin boundary (TB). Although improving the plasticity of γ-TiAl alloy has been paid more attention and great process has been made, it is still insufficient to solve this problem.

Being a special interface defect, TB has been widely studied due to its significant influence on material mechanical property. Nanotwinned materials have attracted a lot of attentions because of their ultrahigh strength and high ductility simultaneously [9,10]. So far, studies of deformation mechanism of nanotwinned metals mainly have focused on face-centered cubic (FCC) metal, such as Cu [11–14], Al [15,16] and Au [17,18]. Besides, the hexagonal closed-packed (HCP) metal are investigated recently, like Mg [19–22]. These studies showed that TB hinders the dislocation glide then strengthens the materials. It can also prevent the dislocation emission from crack tip. The dislocation density around the TB is high, the material is hard, and so the strength of metals is improved [11]. The yield strength of materials relates to both the storage capacity of dislocation and the repulsive force between twinning and dislocation [19]. The studies mentioned above showed that TB in nanocrystalline materials has a great influence on the mechanical property of materials, such as dislocation gliding and the interaction between dislocation and TB. Meanwhile, Wang et al.'s [23] experimental results also illustrated that the interaction between dislocation and TB is a main factor for nanocrystalline metal strengthening.

Crack is one of the major defects that cause the deformation and the failure of materials. It should be pointed out that crack tip plays an important role in crack propagation. A large quantity of research efforts has been devoted to the microstructure and the stress field in crack tip [11,24,25]. Recently, the dislocation nucleation from crack tip in metal materials has been investigated [11]. Strength and ductility are two very important characteristics in the engineering application, while increases of alloy strength are usually accompanied by concomitant decreases of ductility [26]. Therefore, further effort is required to obtain high strength and good ductility of materials simultaneously. Zhou et al. [21] studied the mechanisms of crack propagation in two different crack positions of nanotwinned magnesium. Their results revealed that the left boundary crack turns into brittle cleavage after the plastic propagation. Atoms of the right boundary crack tip are decohered to create a new free surface, which cause the brittle cleavage directly. The emission of dislocation will influence the crack propagation, and TB will hinder the dislocation motion. Sun et al. [11] described the deformation and failure mechanisms of nanotwinned copper with crack. Their study result showed that the crack propagation would be dependent on the crack positions.

For the deformation and failure of nanotwinned materials, these studies still concentrates on Cu and Al materials, while few attentions are paid on the mechanisms of crack propagation in γ-TiAl alloy with pre-existing TB. It is an effective approach to add numbers of TB in γ-TiAl alloy in order to enhance the strength, plasticity and creep ability simultaneously. The mechanical property of γ-TiAl alloy can be improved through controlling the number of TB [27]. As a lamellar interface, TB will hinder the dislocation motion [28]. However, the twin structures and deformation mechanisms have not been considered in experiments, which have great effects on γ-TiAl alloy. The efforts on the essence of deformation and failure mechanism of γ-TiAl alloy with TB should be made to understand in the future. In order to explain the deformation and failure mechanisms of materials and to ameliorate the plasticity at room temperature, it is necessary to use the molecular dynamics (MD) simulation to reveal the competition and interaction between cracks and TB in γ-TiAl alloy from atomic scale.

It has been found that the dislocation motion, TB glide and microstructure of crack tip play very important roles in deformation and failure mechanism of the other metal materials. These study results would be good references in the study of γ-TiAl. Thus, the mechanical properties, mechanisms of deformation and failure in γ-TiAl specimen with crack and TB are elucidated by using dislocation theory and crystal plasticity in this paper. The effects of the crack position on the deformation and failure mechanisms of γ-TiAl specimen with TB are analysed through the snapshots of crack propagation, microstructure of crack tip and stress-strain curves. It would provide guidance for the design and manufacture of high quality γ-TiAl.

2 Construction of modelling

MD simulation model of twin plane in γ-TiAl alloy is built by using Large Scale Atomic/Molecular Massively Parallel Simulator (LAMMPS) package. X, Y and Z are oriented along [111], [11$\bar{2}$] and [$\bar{1}$10] direction, respectively. Cracks prefer to nucleate on TB according to the result of experiment [4]. Thus, three types of crack are employed, namely the lower boundary crack, upper boundary crack and center crack by removing several atom layers along the TB as shown in Figure 1. The model dimension is 22 nm×50 nm ×5 nm with a total of 353088 atoms. An initial crack with 1 nm×5 nm×5 nm is fabricated in each sample. Free boundary conditions are employed in the direction of X and Y, and periodic boundary condition is applied to the direction of Z.

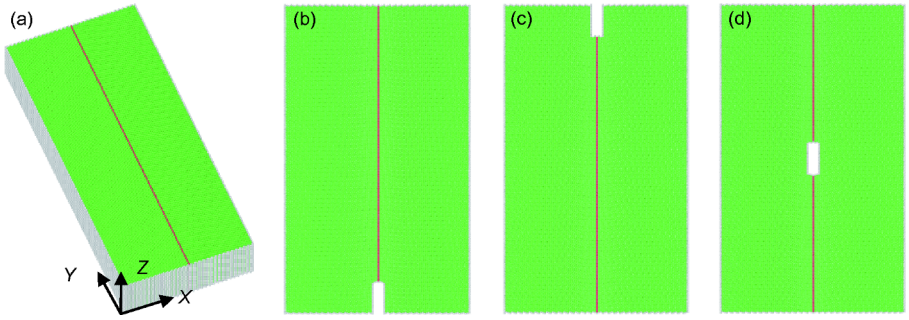

Figure 1 (Color online) Atomic models with different crack positions of γ-TiAl sample. (a) Crack-free structure; (b) lower boundary crack; (c) upper boundary crack; (d) center boundary crack.

In this paper, the crack propagation mechanisms of γ-TiAl specimen with pre-existing TB and cracks of different positions are studied. The motivation is to investigate the deformation and failure mechanisms and to improve the plasticity of γ-TiAl alloy at room temperature. Therefore, the temperature is maintained at 300 K by using the Nose-Hoover thermostat. The MD simulation is conducted in constant NVT ensemble with Velocity-Verlet integrator. The embedded atom method (EAM) [29] is applied to calculate the interatomic interaction force. The potential fitted to both experimental and first-principles data of various crystal properties and structures in Ti-Al system could give a good description of basic properties such as point defects, planar fault energies and elastic constants [30]. After introducing cracks in γ-TiAl specimen with TB, the initial simulation system is relaxed for 100ps to achieve the equilibrium state. Then, uniaxial tension are carried out by applying velocity to atoms in the fixed layers at the right boundary along the X direction, while the fixed layers at the left boundary are free. The tensile strain rate is 4×10^{8} s^{-1}.

The center symmetry parameters (CSP) and common neighbour analysis (CNA) method are used to observe the disorder phenomenon and atom positions of local lattice, which can be visualized by open visualization tool (OVITO). Thus, diverse atomic structures can be distinguished by the different colours. For example, red represents the HCP structure, green stands for the FCC structure and white indicates disordered atoms, which does not belong to any basic atomic structure. Because the structure of γ-TiAl alloy is face-centered tetragonal (FCT), which is similar to the FCC structure, it can be identified as FCC structure in OVITO.

3 Simulation results and discussion

3.1 Process of pre-existing crack propagation with different positions

Crack propagation and fracture are extremely complicated phenomenon, which are caused by atomic bond fracture and dislocation emission from crack tip [31]. The crack propagation is mainly determined by the crack surface energy and the variable slip system of the crack tip [32]. {111} close-packed plane in γ-TiAl alloy has relatively low surface energy, therefore it is the main slip plane. The crack in the bottom of sample shows ductile-brittle transition, which is caused by the TB, the crack tip failure and the competition among dislocation, vacancy and stacking fault (SF). The result is in good consistent with the observation of Sun et al. [11].

In Figure 2(b), with the release of accumulated strain energy, $\frac{1}{6}[12\bar{1}]$ Shockley partial dislocation is observed to emit from the crack tip firstly and glides along ordinary dislocation slip plane {111}, which is in agreement with experiment result [33]. The dislocation propagation could enhance the plasticity of γ-TiAl specimen with TB. As the dislocation motion, the defect on the twin plane causes void generation in the position being close to the crack tip. The coalescent of voids is dominant to the deformation and failure mechanisms. A large number of intrinsic stacking fault (ISF) and extrinsic stacking fault (ESF) can be observed in Figure 2(c). ISF stands for two layers of HCP atom and ESF has a layer of FCC atom between two layers of HCP atom. The atomic plane slip is caused by the reaction and motion of dislocations in different slip planes. It results in the destruction of the original periodic stacking sequence of atoms. As a result, ISF and ESF are formed.

As the applied strain increases, TB being a dislocation source will emit dislocation, and new Shockley dislocation nucleates from the slip plane close to ISF. Therefore, the generation of dislocation and the interaction among dislocations will increase accordingly. It causes that the atomic plane slips to be easier and the SF generated previously propagates. It can be observed in Figure 2(e) and (f) that the ISF changes to ESF resulting from partial dislocation gliding. Subsequently, it can be shown in Figure 2(d) that the void in black circle is caused by the dislocation emission and the stress concentration because of SFs piled-up in boundary. Moreover, the new SF, defined as secondary SF, would form in the existed ISF and ESF. Two partial dislocations in the

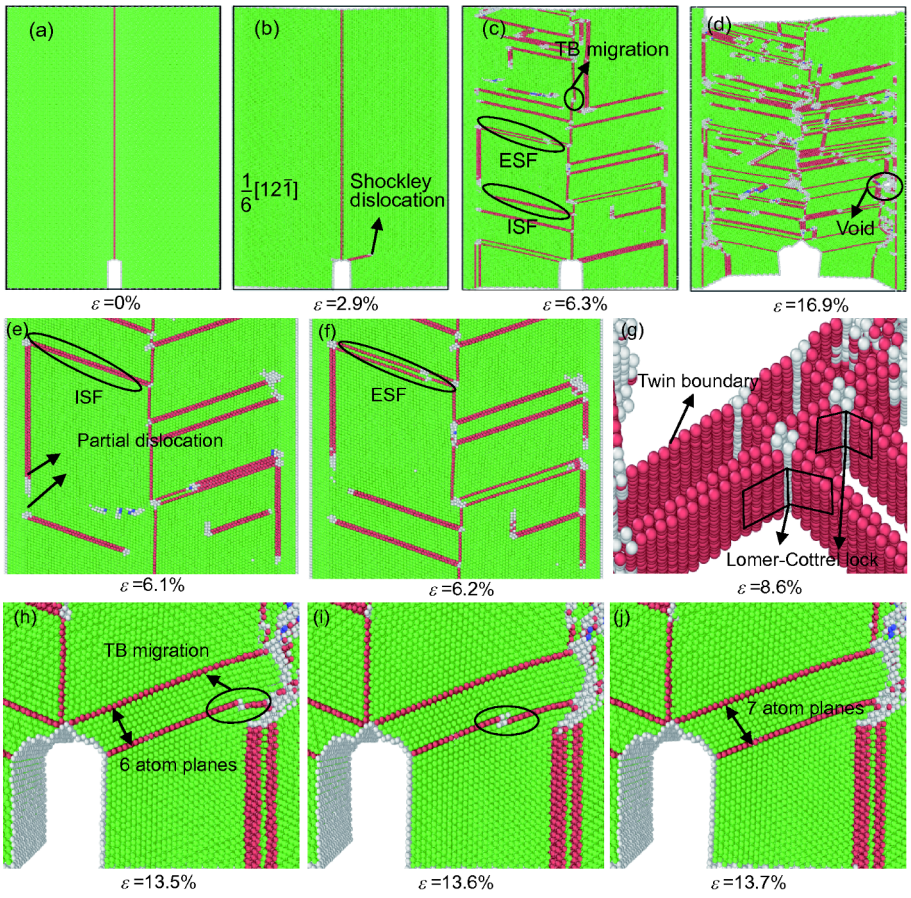

Figure 2 (Color online) Propagation process of lower boundary crack. (a) Initial configuration; (b) the first dislocation emits; (c) a large number of ISF and ESF form; (d) the coherency loss of twin boundary and void generation in boundary; (e) partial dislocation ahead of SFs; (f) ISF changes to ESF; (g) Lomer-Cottrell dislocation; (h), (i) and (j) are the TB migration progress.

junction of close-packed planes react to form a stair-rod dislocation. The stair-rod dislocation connects two SFs and forms Lomer-Cottrell lock, which is shown in Figure 2(g). Lomer-Cottrell lock usually hinders the motion of other dislocations because of its stability. The dislocation types of γ-TiAl at room temperature are mainly $\frac{1}{2}\langle 110]$ ordinary dislocation and $\langle 101]$ superdislocation. The perfect dislocation in the close-packed plane will dissociate to be partial dislocations, such as:

$$\frac{1}{2}[10\bar{1}] \rightarrow \frac{1}{6}[11\bar{2}] + \frac{1}{6}[2\bar{1}\bar{1}]. \quad (1)$$

With the special microstructure of γ-TiAl, $L1_0$ atomic ordering, it would affect the structure of dislocation. Thus, the generated dislocation of these types would be different with FCC metals. However, the partial dislocations $\frac{1}{6}[11\bar{2}]$, $\frac{1}{6}[1\bar{2}1]$ and $\frac{1}{6}[\bar{2}11]$ are all equivalent in FCC metals, but are not equivalent due to the poor symmetry of γ-TiAl. The generation of ISF, ESF, stair-rod lock and Lomer-Cottrell lock has close relationship with dislocations, because the difference of dislocation type resulting in these defects structure of γ-TiAl are different with that of FCC metals. However, their generation mechanisms are similar. Partial dislocations will meet and form dislocation locks continually. The strength of γ-TiAl specimen with TB can be improved by the interaction of these dislocations. With increasing strain, new dislocations nucleate and multiply continually. The existed active dislocations will annihilate or disappear partially because of the reactions among dislocations. Owing to the coalescence of SFs, structure transformations from initial FCT structure to HCP structure are obtained. SFs and structure transformations are the main plastic deformation mechanisms in lower boundary crack model. On the one hand, TB plays the role of repulsion when the dislocation moves towards the TB, and the glide of dislocation in γ-TiAl specimen will be hindered by this repulsive force. On the other hand, owing to the tension force application on dislocations and the repulsive force between adjacent dislocations cause dislocations glide. Finally, dislocations are hindered by the TB. They cause the pile-up of dislocations around the TB. The high dislocation density around TB hardens the material, so as to improve the strength

of metals [11]. It is important to highlight that when the local accumulated dislocations on the TB reach a saturation point, the dislocations on the same or adjacent close-packed planes would continue to move towards the TB and dissociate. It can be seen in Figure 2(c) that the one passes across the boundary and glides, and the other moves along the TB causing TB migration, and finally destroys the coherency structure of the TB. This result is in agreement with that of experiment [34] and similar to the observation of other metals [35,36]. Because the dislocation pile-up leads to the deformation of the material, it plays a crucial role on retaining ductility of γ-TiAl specimen.

The fabricated twin is defined as primary twin and the twin generated later as secondary and tertiary twins. As strain increases, SFs around crack tip or other locations transmits into twin. The generation of secondary and tertiary twins indicates that the motion of twinning partial is faster than the tailing partial does in the SF. For the primary twin serving as an effective barrier for the secondary twins, the secondary twins would not passing across the primary twin, and the same to the tertiary twins. This mechanism contributes to strain hardening during plastic deformation [37]. During the whole deformation process, the deformation mechanism occurred on secondary twins is TB migration far more than the dislocation emission. It can be inferred that the stress needed for dislocation emission is higher than that of TB migration. Furthermore, the TB migration can also be observed around crack tip, and it would add an atom plane. The evolution is showed in Figure 2(h) to (j). It can be seen from the evolution process of three cracks that the blocking effect of secondary and tertiary twins on crack would increase with their increasing spacing and density. As a result, the ductility of γ-TiAl specimen would enhance. Although the FCT structure of γ-TiAl is very similar to FCC structure metals, because of its poor symmetry and low stacking fault energy, it is easier to generate twin than FCC metals.

Moreover, the dislocation motion will also be hindered by the dislocation reaction and SF resulting from dislocation motion. Because of the special structure of γ-TiAl, it is harder for dislocation to move than FCC metals. These is a consequence of strong atomic bonding owing to covalent rather than metallic bonding, which makes dislocation motion through the crystalline structure difficulty.

The crack tip blunting and the ductility mechanism of γ-TiAl result in the crack propagation along the length direction to be slower than that of the width direction. The crack starting to propagate along [010] direction is induced by the metallic bond fracture of the crack tip atom. An interesting finding is that the crack doesn't propagate before the coherency structure of TB is destroyed. It can be speculated that TB can hinder the crack propagation. The crack would propagate more slowly after twin generates at crack tip. The appearance of twin and activity of dislocations would inhibit crack propagation. In addition, the hierarchical twin of γ-TiAl provides additional blocks of dislocation movement for strengthening materials.

Microcrack nucleation and crack propagation in a near lamellar γ-TiAl alloy was investigated in 4-point bend specimens using selected area channelling patterns and electron channelling contrast imaging indicated that extensive twinning and dislocation activity inhibit crack propagation [38]. Besides, Huang et al. [39] studied the crack propagation by using transmission electron microscopy, they found that twins and microcracks generated during crack growth. These results are in agreement with simulation results in this work. It is very difficult for dislocation to nucleate without active slip plane at the crack tip. If the crack tip doesn't have active slip system, the crack prefers to propagate in a brittle manner [31]. It has been found in the previous study [40] that the crack of γ-TiAl without TB propagates in the manner of brittle cleavage fracture rapidly at room temperature. It is very different from the crack propagation of the sample with TB in this paper, which indicates that the TB will influence the crack propagation mechanism. The other ductility mechanism of γ-TiAl is that the instability of crack will cause crack deflection during the crack propagation process [41]. The crack deflection will release more strain energy and it is an effective mechanism of resisting deformation. The result is similar to that of experiment [42]. Of course, the crack deflection will also improve the fracture toughness of γ-TiAl specimen with TB.

Partial dislocations in different slip planes react to form the stacking fault tetrahedral (SFT) shown in Figure 3. The Thompson tetrahedron is introduced to illustrate the dislocation reaction during the evolution of SFT. The evolution of SFT is shown as following.

The dissociation reaction of Frank partial dislocation is

$$\frac{1}{3}[111] \rightarrow \frac{1}{6}[101] + \frac{1}{6}[121]. \tag{2}$$

Frank dislocation loop αA dissociates into Shockley partial dislocation from its slide planes ACD, ABD and ABC. The dissociation reaction of dislocations is as follows:

$$\alpha A \rightarrow \alpha\beta + \beta A, \text{ (In ACD plane)}, \tag{3}$$

$$\alpha A \rightarrow \alpha\gamma + \gamma A, \text{ (In ABD plane)}, \tag{4}$$

$$\alpha A \rightarrow \alpha\delta + \delta A, \text{ (In ABC plane)}. \tag{5}$$

Three stair-rod dislocations CD, BD and CB are generated by the dislocation reaction, and their corresponding Burgers vectors are $\alpha\beta$, $\alpha\gamma$ and $\alpha\delta$ respectively. Meanwhile, three Shockley partial dislocations and three SFs are generated after the dislocation reaction. The Burgers Vectors of the Shockley partial dislocations are βA, γA and δA.

$$\beta A + A\gamma \rightarrow \beta\gamma, \text{ (along DA)}, \tag{6}$$

$$\gamma A + A\delta \rightarrow \gamma\delta, \text{ (along BA)}, \tag{7}$$

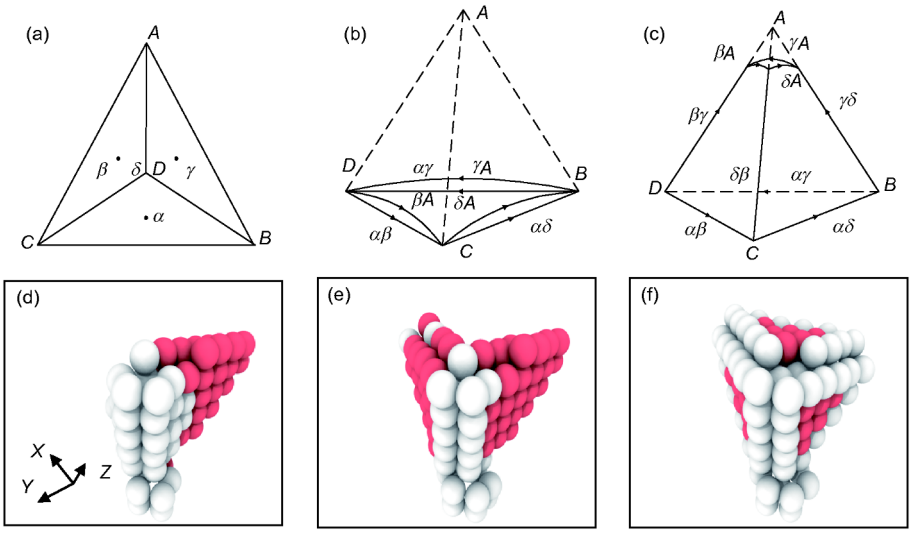

Figure 3 (Color online) Evolution of STF. (a) Thompson tetrahedron; (b) and (c) show the dislocation reaction of the STF; (d), (e) and (f) show the atom configuration of the STF.

$$\delta A + A\beta \rightarrow \delta\beta, (\text{along CA}). \tag{8}$$

Owing to the repulsion of stair-rod dislocations $\alpha\beta$, $\alpha\gamma$ and $\alpha\delta$, the Shockley partial dislocation βA, γA and δA would bend outward along their slip plane. Because of the attractiveness among Shockley partial dislocations, the new stair-rod dislocations $\beta\gamma$, $\gamma\delta$ and $\delta\beta$ are generated. After these dislocation reactions, the triangular Frank dislocation evolves into a stable SFT that comprises four stacking faults and six stair-rod dislocations.

Besides, single vacancies induced by the dislocation motion along the slip system after its reaction are observed. The coordination number of a perfect lattice is 12. The vacancy in Figure 4(d) has 12 atoms, representing that every atom has 11 neighbor atoms. The formation and migration of vacancy can improve the plasticity of samples. This result is in good consistence with that of Xu [43].

To gain a better understanding of the crack propagation mechanism, the evolution process of crack tips need to be analysed. It can be seen from Figures 5–7 that with increasing external load, the atomic bond would fracture resulting in the crack tip atoms being out of order and the dislocation nucleation and emission from the crack tip. The stress concentrates on the crack tip along the slip plane, which is illustrated in Figure 5(g)–(i). Owing to the lattice mismatch, the stress redistribution with the crack propagation is caused by the stress along the TB fluctuation. Holian et al. [44] found stress concentration and dislocations emission from the crack tip. The same result can be obtained from this paper. The crack begins to propagate after the coherency of TB lost completely, it can be seen that the crack tip is in sharp all the time from the Figures 5–7. In Figure 5(e), the void generated ahead of the crack tip is presented.

The crack coalescent with voids is observed in Figure 5(f). Wu et al. [25] revealed that the crack propagation begins with the growing of voids and forming of microcracks at the crack tip. After that, it is the connection between microcracks and the main crack that leads to crack propagation eventually. From the evolution process of crack tips of three samples, it can be seen that a plastic zone existed at crack tip results from dislocation and twin generation. It is agreement with Huang's experiment results [39]. However the dislocation is more common than twin in simulation results and this is disagreement with that of experiment [39]. These can be attributed to different samples and loading method, namely cyclic loading applied on polycrystalline γ-TiAl in experiment and uniaxial tension employed on single γ-TiAl in simulation.

In order to study the crack propagation and the mechanism of dislocation emission with different crack positions, the Rice model [45] was used to calculate energy release rate of the dislocation nucleation from the crack tip. Based on the perfect sharp crack model, the formula of energy release rate is

$$G_{\text{disl}} = \frac{8\gamma_{\text{usf}}\left[1+(1-\nu)\tan^2\phi\right]}{\left[(1+\cos)\sin^2\theta\right]}, \tag{9}$$

where γ_{usf} is the unstable stacking fault energy; ν is the Poisson's ratio of γ-TiAl; ϕ is the angle between Burgers vector and a line in the slip plane perpendicular to the crack front; θ is the angle between the slip plane and the crack surface.

The value of parameters γ_{usf} is taken from the work of Zhou et al. [46].

Cracks employed in the models are not atomically sharp initially, but they possess a sharp crack tip after propagation. Therefore, eq. (9) was used to roughly calculate the energy release rate of upper boundary crack, lower boundary crack

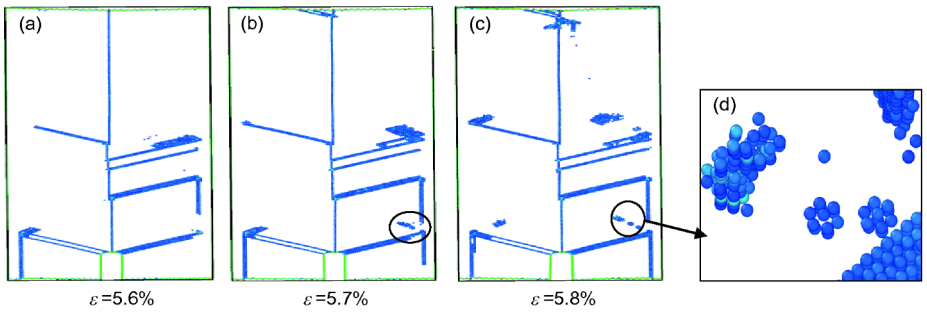

Figure 4 Formation processes of vacancies. (a) Dislocation nucleation; (b) dislocation motion; (c) vacancy formed after dislocation motion; (d) zoomed views of the vacancies.

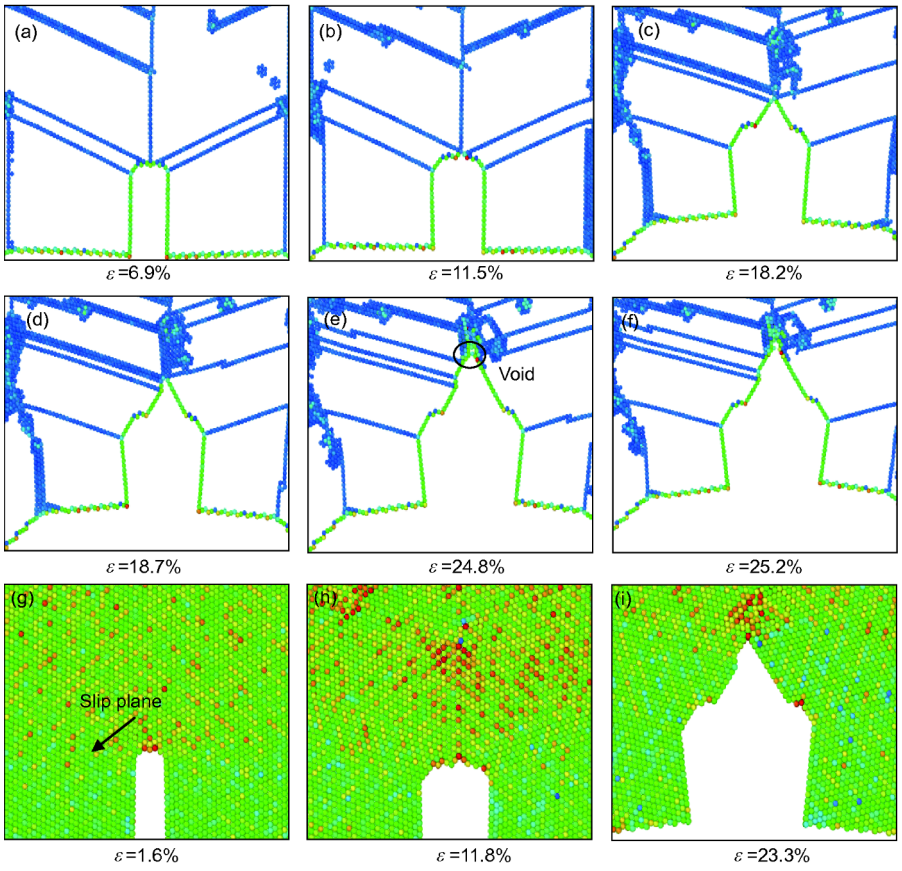

Figure 5 Evolution process of the crack tip of lower boundary crack ((g)–(i), the color scale employed corresponds to stress increasing from blue, the weakest, to red, the strongest).

and center crack. The energy consumed during the dislocation generation process is shown in Table 1. The energy release rates of the dislocation nucleation with three kinds of crack positions are compared. It can be seen in Table 1 that the partial dislocation is favorable to emit from the crack tip of the lower boundary crack.

Rice and Thomson [47] proposed the brittle-ductile criterion by emission dislocations from crack tip and competition mechanism of cleavage manner. Dislocation emissions from the crack tip are observed at the beginning of tension in the crack propagation process. It is visible that the dislocation emission prefers to the crack cleavage propagation. During the crack propagation process, the atom decohesion at the crack tip leads to the crack tip sharpening. From the evolution process of the crack tip of the lower boundary crack model shown in Figure 5, it is found that the crack propagation undergoes a transition from ductile to brittle.

It can be seen from Figure 6 that the evolution process of the crack tip of the upper boundary crack model is obviously distinct from that of the lower boundary crack. The crack tip would be blunted after dislocation emission, while no void occurs. The crack propagates slowly and it is ductile de-

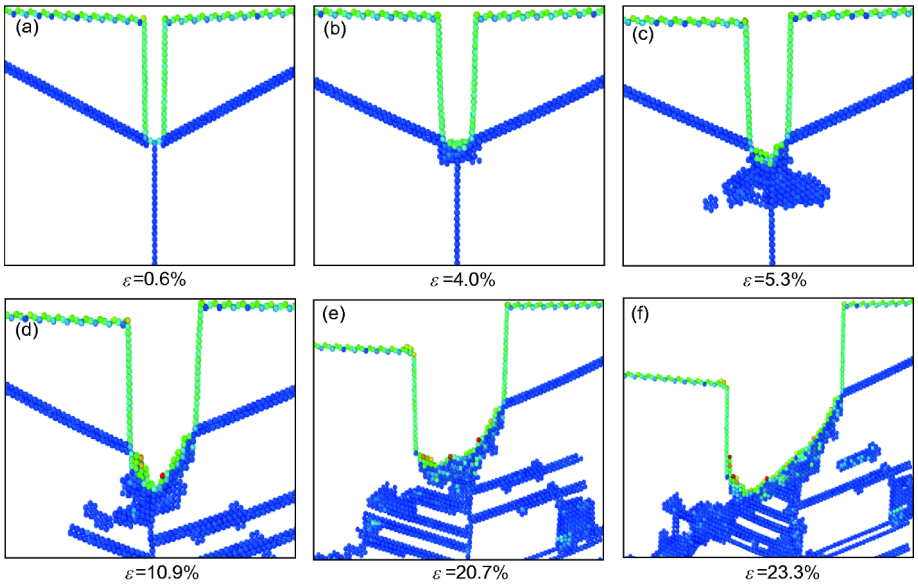

Figure 6 (Color online) Evolution process of the crack tip of upper boundary crack.

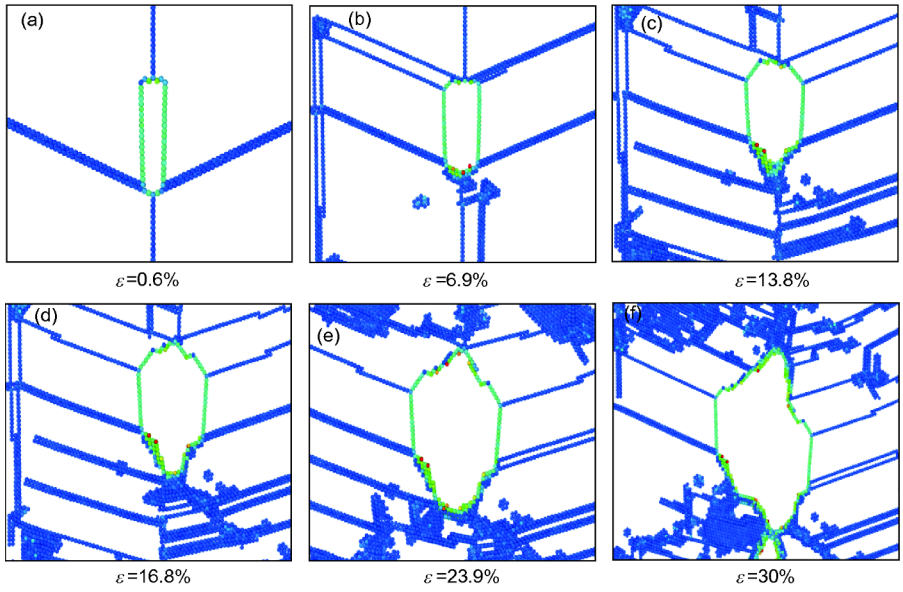

Figure 7 (Color online) Evolution process of the crack tip of center crack.

Table 1 Energy consumed during dislocation generation process

Crack	γ_{usf} (J m^{-2})	ϕ	ν	θ	G_{disl} (J m^{-2})
Upper	1.97	0	0.26	112	29.34
Lower	1.97	0	0.26	68	13.34
Center	1.97	0	0.26	112	29.34

formation rather than brittle deformation. Because the dislocation emission from the crack tip takes priority over crack cleavage propagation, the specimen is followed with toughness fracture finally.

Figure 7 demonstrates that the evolution process of the crack tip of the center crack model isn't similar to those of the upper boundary and the lower boundary crack models. The crack propagates initially along the direction of [0$\bar{1}$0], and then the crack tip blunts in this direction after the dislocation nucleates. It does not exhibit the phenomenon of sharpening, which resembles the evolution process of the crack tip of the upper boundary crack model.

Then the crack propagates in the direction of [010], and the crack tip in this direction blunts firstly and is followed by sharpness. It is similar to the crack evolution process of the lower boundary crack, because energy release rate resembles both in the center crack and the upper boundary crack models. The same energy release rate indicates that the difficulty degree of the dislocation emission from the crack tip is same as each other. Because the center crack propagates both along the $[0\bar{1}0]$ and [010] direction, it leads to that this specimen fractures faster than the other two crack specimens. Because of the dislocation existing around the crack tip, the crack only propagates a short distance along the TB. The propagation of the lower boundary crack in this paper agrees with that of Zhou et al. [21], who found that the crack propagation of the left boundary crack also undergoes the transition from ductile to brittle. During the entire process of crack propagation, there is less dislocation emission at the crack tip of right boundary crack. The crack tip is sharp from the initial propagation. The result is disagreement with that of this paper. Because the γ-TiAl specimen used in this paper is the FCT structure and the magnesium sample being the HCP structure in Zhou's work, and the microstructure of the crack tip varies in the process of crack propagation with the lattice structure. The mechanisms of crack propagation are not exactly the same among three kinds of crack position because of the diversity evolution of microstructures at crack tips. In addition, the discrepancy of crack propagation mechanism can also be attributed to the anisotropy of the crystal [30,48].

3.2 Stress-strain curves with different crack positions

In order to explain the mechanism of deformation and fracture failure further, the typical stress-strain curves with different crack positions are given in Figure 8. The stress would increase rapidly with increasing strain, however, there is not remarkable difference observed on the elastic deformation stage of three curves. When the strain increases to a critical value, the stress also reaches the maximum value. It can be seen from zoom view of stress-strain curves that the maximum stress of the lower boundary crack and the upper boundary crack are 5.76 and 5.80 GPa respectively. They are obviously larger than the maximum stress 5.08 GPa of the center crack, it means that the strength and plasticity are significantly higher than the center crack.

In Figure 9, it can be concluded that the trend of strength increase from the points of A_l to B_l, A_u to B_u and A_c to B_c. Based on the atomic configuration corresponding to these points, the strength increase is caused by the generation, spacing and density of the secondary and tertiary twins. It can be seen clearly that the location and density of secondary and tertiary twins are different owing to the different stress field of three crack position. Furthermore, there is a competition between hierarchical twin and crack propagation, for the hierarchical twin being dominant the main plastic deformation mechanism, the crack propagation would be slow down. And hierarchical twin can effectively prevent dislocation further movement, therefore, the ductility of γ-TiAl specimen enhances.

Of course, secondary and tertiary twins are not the only factor effecting strength. It is noted that the dislocation nucleation needing enough stress leads to the increase of stress. The dislocation emission will consume a part of the stress, so that the stress decreases. It should be pointed out that dislocations emission continually both from the crack tip and the TB can be observed. Owing to the boundary obstructed the dislocation, there is insufficient room for dislocation to move, and finally accumulates on the boundary. The piling up of dislocations also increases the stress, and the SF resulting from the dislocation motion also releases the stress [24]. It causes the stress-strain curve fluctuates. Because of the obstructive effect of the TB on the dislocation motion, the partial dislocations would be pinned at the TB and their motion would be restricted when they move to the TB [49]. This is the strengthening effect of TB on the plastic deformation stage of the γ-TiAl specimen. Some dislocations are pinned on the TB and arrested by the TB to form new

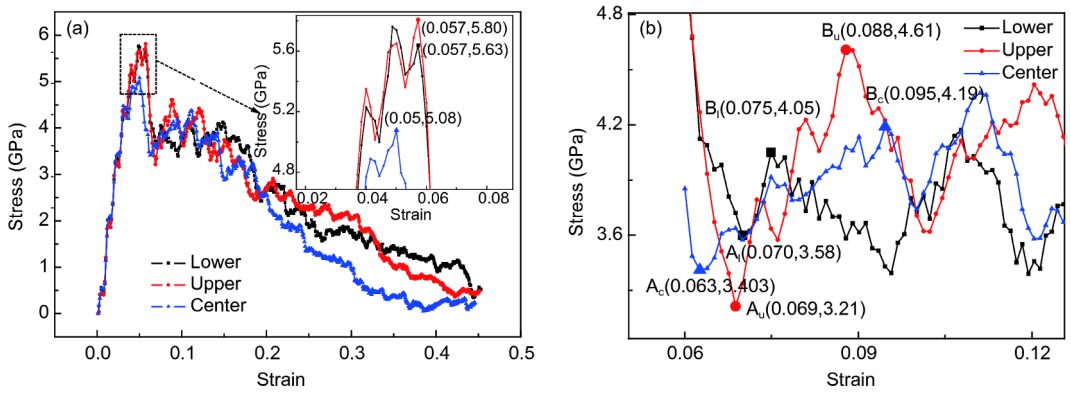

Figure 8 (Color online) Stress-strain curves with different crack positions.

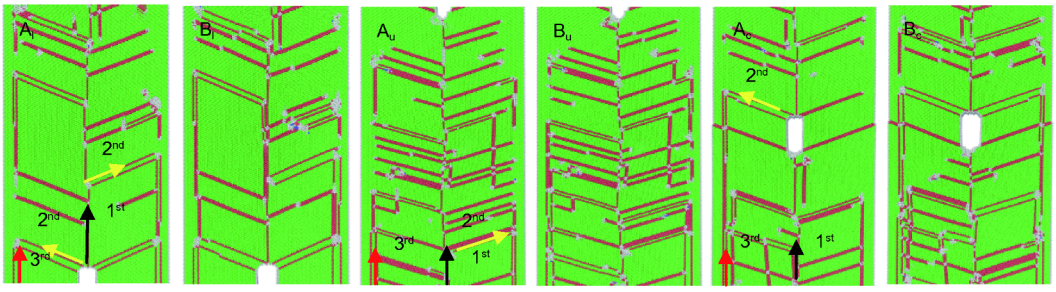

Figure 9 Parts of stress-strain curves (strain from 6% to 12.5%) with different crack positions and the atomic configuration corresponding to the points scaled in stress-strain curves (A_l and B_l stands for the points of lower boundary crack model, A_u and B_u stands for the points of upper boundary crack model, A_c and B_c stands for the points of center boundary crack model, 1st, 2nd and 3rd represents primary twins (black arrows), secondary twins (yellow arrows) and tertiary twins (red arrows) respectively).

partial dislocations. They lead to steps generation at the TB, which in turn becomes a new source of dislocation. These partial dislocations can glide along the TB, which are both beneficial to release the stress concentration generated by dislocation accumulation and to improve the ductility of γ-TiAl specimen. Curves of the lower boundary, the upper boundary and the center crack begin to drop sharply at ε=5.7%, ε=5.7% and ε=5.0% respectively. It means that the center boundary crack is the most likely to propagate, followed by the lower and upper boundary cracks. It is consistent with the phenomena observed in the atomic configuration. The center crack results in γ-TiAl specimen with TB fracture quickly than the other models. The average flow stress shown in Table 2 under different crack positions was calculated. It is shown clearly that the average flow stress is the smallest of center crack. In other words, the ductility of γ-TiAl specimen containing center crack is the worst, following the upper boundary crack and lower boundary crack.

It can be found through the above analysis that the largest difference of γ-TiAl with other FCC metals is that the movable slip system of γ-TiAl is less than the other FCC metals, leading to the dislocation of γ-TiAl hard to move. The crack propagation mechanism of FCC metals is mainly the competition between dislocation emission and crack propagation, while competition among dislocation emission, crack propagation and hierarchical twin is the main deformation mechanism of γ-TiAl.

4 Conclusions

MD is employed to investigate the deformation and failure mechanism of γ-TiAl specimen with pre–existing crack and TB. Simulation results revealed that the nature of the deformation behaviour is mainly the reaction of dislocation-dislocation, dislocation-twin and twin-twin. The formation of the secondary twins and tertiary twins suggests a hierarchical twin deformation mechanism that leads to the strength enhancement with non-compromising ductility and strain hardening. The lower boundary crack and the center crack undergo a ductile-brittle transition during the propagation according to the energy release rate of the dislocation nucleation from the crack tip and the atomic configuration. Their yield strength is different according to the stress-strain curves. The yield strength of the upper boundary crack is the highest, following the lower boundary crack and the center crack. The dislocation behaviour, SFs and hierarchical twin with different crack positions are the decisive factors for the yield strength. In addition, the pre-existing TB would affect the propagation mechanism of crack, hinder the motion of dislocations and promote dislocation accumulation and crack deflection, this can prevent the crack from propagating and improve fracture toughness. The simulation results can also show that the motion of dislocation, the formation of SFs, secondary and tertiary twins play very important roles in the deformation and the failure process. The type of dislocation, the vacancy formed by the dislocation motion and SFs and the dislocation lock can affect the plasticity of the specimen.

Table 2 The average flow stress under different crack positions (the average flow stress was calculated from a strain of 6% to 33%)

Model	Stress (GPa)
Upper boundary crack	2.64
Lower boundary crack	2.76
Center boundary crack	2.20

This work was supported by the National Natural Science Fundation of China (Grant Nos. 51665030, 51865027), the Program for Changjiang Scholars and Innovative Research Team in University of Ministry of Education of China (Grant No. IRT_15R30), and the Doctoral Research Foundation of Lanzhou University of Technology.

1 Clemens H, Mayer S. Design, processing, microstructure, properties, and applications of advanced intermetallic TiAl alloys. Adv Eng Mater, 2013, 15: 191–215
2 Marketz W T, Fischer F D, Clemens H. Deformation mechanisms in TiAl intermetallics—experiments and modeling. Int J Plasticity, 2003, 19: 281–321
3 Clemens H, Smarsly W. Light-weight intermetallic titanium aluminides—status of research and development. AMR, 2011, 278: 551–

556
4 Bieler T R, Fallahi A, Ng B C, et al. Fracture initiation/propagation parameters for duplex TiAl grain boundaries based on twinning, slip, crystal orientation, and boundary misorientation. Intermetallics, 2005, 13: 979–984
5 Wang H, Xu D S, Yang R. Implementing large-scale parallel atomistic simulations in the investigation of interfacial behaviors in titanium alloys (in Chinese). e-Sci Tech Appl, 2013, 33: 139–152
6 Kim Y W. Ordered intermetallic alloys, part III: Gamma titanium aluminides. JOM, 1994, 46: 30–39
7 Chen G, Peng Y, Zheng G, et al. Polysynthetic twinned TiAl single crystals for high-temperature applications. Nat Mater, 2016, 15: 876–881
8 Forwood C T. Slip transfer of deformation twins in duplex γ-based Ti-Al alloys. Part I. Transfer across γ-γ coherent twin interfaces. Philos Mag A, 2000, 80: 2747–2783
9 Zhao X, Lu C, Tieu A K, et al. Deformation mechanisms in nanotwinned copper by molecular dynamics simulation. Mater Sci Eng-A, 2016, 687: 343–351
10 Kou H, Lu J, Li Y. High-strength and high-ductility nanostructured and amorphous metallic materials. Adv Mater, 2014, 26: 5518–5524
11 Sun L G, He X Q, Wang J B, et al. Deformation and failure mechanisms of nanotwinned copper films with a pre-existing crack. Mater Sci Eng-A, 2014, 606: 334–345
12 Wei Y. Scaling of maximum strength with grain size in nanotwinned fcc metals. Phys Rev B, 2011, 83: 132104
13 Zheng Y G, Zhang H W, Chen Z, et al. Roles of grain boundary and dislocations at different deformation stages of nanocrystalline copper under tension. Phys Lett A, 2009, 373: 570–574
14 Wang Y M, Sansoz F, LaGrange T, et al. Defective twin boundaries in nanotwinned metals. Nat Mater, 2013, 12: 697–702
15 Xie Y H, Xu J G, Song H Y, et al. Effect of twin boundary on nanoimprint process of bicrystal Al thin film studied by molecular dynamics simulation. Chin Phys B, 2015, 24: 026201
16 Gao L, Song H Y, Sun Y, et al. Effects of twist twin boundary and stacking fault on crack propagation of nanocrystal Al. Comput Mater Sci, 2014, 95: 484–490
17 Wen Y H, Wang Q, Liew K M, et al. Compressive mechanical behavior of Au nanowires. Phys Lett A, 2010, 374: 2949–2952
18 Deng C, Sansoz F. Near-ideal strength in gold nanowires achieved through microstructural design. ACS Nano, 2009, 3: 3001–3008
19 Song H, Li Y. Effect of twin boundary spacing on deformation behavior of nanotwinned magnesium. Phys Lett A, 2012, 376: 529–533
20 Guo Y F, Xu S, Tang X Z, et al. Twinnability of hcp metals at the nanoscale. J Appl Phys, 2014, 115: 224902
21 Zhou L, Guo Y F. Dislocation-governed plastic deformation and fracture toughness of nanotwinned magnesium. Materials, 2015, 8: 5250–5264
22 Song B, Guo N, Liu T, et al. Improvement of formability and mechanical properties of magnesium alloys via pre-twinning: A review. Mater Des (1980-2015), 2014, 62: 352–360
23 Wang J, Li N, Anderoglu O, et al. Detwinning mechanisms for growth twins in face-centered cubic metals. Acta Mater, 2010, 58: 2262–2270
24 Guo Y F, Wang C Y, Zhao D L. Atomistic simulation of crack cleavage and blunting in bcc-Fe. Mater Sci Eng-A, 2003, 349: 29–35
25 Wu W P, Yao Z Z. Molecular dynamics simulation of stress distribution and microstructure evolution ahead of a growing crack in single crystal nickel. Theor Appl Fract Mech, 2012, 62: 67–75
26 Wu Z X, Zhang Y W, Srolovitz D J. Deformation mechanisms, length scales and optimizing the mechanical properties of nanotwinned metals. Acta Mater, 2011, 59: 6890–6900
27 Morris M A, Leboeuf M. II. Deformed microstructures during creep of TiAl alloys: Role of mechanical twinning. Intermetallics, 1997, 5: 339–354
28 Teng C Y, Zhou N, Wang Y, et al. Phase-field simulation of twin boundary fractions in fully lamellar TiAl alloys. Acta Mater, 2012, 60: 6372–6381
29 Zope R R, Mishin Y. Interatomic potentials for atomistic simulations of the Ti-Al system. Phys Rev B, 2003, 68: 024102
30 Xu D, Wang H, Yang R, et al. Molecular dynamics investigation of deformation twinning in γ-TiAl sheared along the pseudo-twinning direction. Acta Mater, 2008, 56: 1065–1074
31 Zhou Y, Yang Z, Lu Z. Dynamic crack propagation in copper bicrystals grain boundary by atomistic simulation. Mater Sci Eng-A, 2014, 599: 116–124
32 Zhou M. A new look at the atomic level virial stress: On continuum-molecular system equivalence. Proc R Soc A-Math Phys Eng Sci, 2003, 459: 2347–2392
33 Simkin B A, Ng B C, Crimp M A, et al. Crack opening due to deformation twin shear at grain boundaries in near-γ TiAl. Intermetallics, 2007, 15: 55–60
34 Hao Y, Liu J, Li S, et al. Effects of nano-twinning on the deformation and mechanical behaviours of TiAl alloys with distinct microstructure at elevated loading temperatures. Mater Sci Eng-A, 2017, 705: 210–218
35 Song H Y, Li Y L. Atomic simulations of effect of grain size on deformation behavior of nano-polycrystal magnesium. J Appl Phys, 2012, 111: 044322
36 Song H Y, Sun Y. Effect of coherent twin boundary and stacking fault on deformation behaviors of copper nanowires. Comput Mater Sci, 2015, 104: 46–51
37 Wei Y, Li Y, Zhu L, et al. Evading the strength-ductility trade-off dilemma in steel through gradient hierarchical nanotwins. Nat Commun, 2014, 5: 3580
38 Ng B C, Simkin B A, Crimp M A, et al. The role of mechanical twinning on microcrack nucleation and crack propagation in a near-γ TiAl alloy. Intermetallics, 2004, 12: 1317–1323
39 Huang Z W, Bowen P, Jones I P. Transmission electron microscopy investigation of fatigue crack tip plastic zones in a polycrystalline γ-TiAl-based alloy. Philos Mag A, 2001, 81: 2183–2197
40 Fu R, Rui Z Y, Yan C F et al. Molecular dynamics simulation of micro-crack propagation behavior in single crystal γ-TiAl (in Chinese). J Funct Mater, 2015, 46: 13100–13105
41 Yamakov V, Saether E, Phillips D R, et al. Dynamic instability in intergranular fracture. Phys Rev Lett, 2005, 95: 15502–15700
42 Mine Y, Takashima K, Bowen P. Effect of lamellar spacing on fatigue crack growth behaviour of a TiAl-based aluminide with lamellar microstructure. Mater Sci Eng-A, 2012, 532: 13–20
43 Xu S, Guo Y F, Wang Z D. Deformation mechanism of the single-crystalline nano-Cu films: Molecular dynamics simulation. Comput Mater Sci, 2013, 67: 140–145
44 Holian B L, Ravelo R. Fracture simulations using large-scale molecular dynamics. Phys Rev B, 1995, 51: 11275–11288
45 Rice J R. Dislocation nucleation from a crack tip: An analysis based on the Peierls concept. J Mech Phys Solids, 1992, 40: 239–271
46 Zhou Z R, Wang Y, Xia Y M. Molecular dynamics study of deformation mechanism of γ-TiAl intermetallics. Acta Phys Sin-Ch Ed, 2007, 56: 1526–1531
47 Rice J R, Thomson R. Ductile versus brittle behaviour of crystals. Philos Mag, 1974, 29: 73–97
48 Yamakov V, Saether E, Phillips D R, et al. Molecular-dynamics simulation-based cohesive zone representation of intergranular fracture processes in aluminum. J Mech Phys Solids, 2006, 54: 1899–1928
49 Wang G M. Molecular Dynamics Simulation of the Mechanical Behavior of Nanotwinned Copper (in Chinese). Dissertation for Master Degree. Hangzhou: Zhejiang University, 2011